

Hybrid NMR: A Union of Solution and Solid-State NMR

Supporting Information

Pallavi Thiagarajan-Rosenkranz, Adrian W. Draney and Justin L. Lorieau*

Department of Chemistry, University of Illinois at Chicago, 845 W Taylor St, Chicago IL

60607

* Corresponding Author: justin@lorieau.com

Distribution of crystal orientations and symmetric tensors. We were able to characterize the distribution in polar angles (β) for the crystallite orientations with respect to the laboratory frame from the $^2\text{H}_2\text{O}$ quadrupolar powder lineshape. Based on the fit of the PRO ^2H spectrum in Figure 1, we found that our samples are uniformly and spherically distributed in the β angle. However, the $^2\text{H}_2\text{O}$ quadrupolar tensor is expected to be axially symmetric, and this spectrum cannot be used to determine the crystallite distribution in the azimuthal angle, α .

The average tensor measured in a uniformly distributed PRO sample is described as follows (from equation (16)):

$$V_{20}^{(LAB)} = \sum_m V_{2m}^{(AVE)} \mathcal{D}_{m0}^{AL} \quad (\text{S1})$$

The final spectrum is integrated over the crystallite β^{AL} and α^{AL} angles from the five Wigner components, \mathcal{D}_{m0}^{AL} . In the more general case, the β and α angles may deviate from a uniform spherical distribution if the crystallites are locked in the hydrogel in a non-uniform distribution.

$$V_{20}^{(LAB)} = \sum_m V_{2m}^{(AVE)} \mathcal{D}_{m0}^{AL} P(\alpha) P(\beta) \quad (\text{S2})$$

This deviation is represented by a probability distribution, $P(\alpha)$ and $P(\beta)$, for the two angles. This expression assumes that the distribution functions in crystallite β and α angles are not correlated.

We were able to avoid a non-uniform distribution, at least in the β angle, by reprocessing our samples. However, it is not possible, without rotating the sample about a vector orthogonal to the B_0 field, to determine the crystallite distribution in α angles from an axially symmetric (or nearly axially symmetric) tensor, like the quadrupolar coupling

tensor of $^2\text{H}_2\text{O}$. For an axially symmetric tensor, the $m=\pm 2, \pm 1$ terms are equal to zero, and equation (S2) only depends on the β angle.

$$V_{20}^{(LAB)} = \sum_m V_{20}^{(AVE)} d_{00}^{AL}(\beta) P(\beta) \quad (\text{S3})$$

Likewise, a non-uniform distribution in the azimuthal angle cannot make an axially symmetric tensor appear axially asymmetric. The above does not hold true if the distributions in α and β angles are correlated such that $P(\alpha, \beta)$. However, in this case, the spectrum of symmetric tensors would all appear axially asymmetric, including the ^2H spectrum of $^2\text{H}_2\text{O}$.

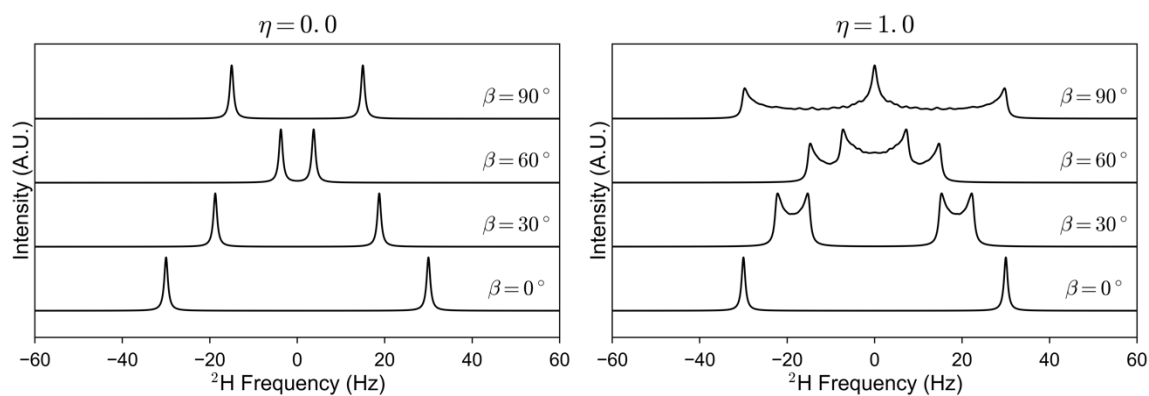


Figure S1. Simulated ^2H spectra for a biaxial liquid crystal ordered along the β_{CL} angle and statically disordered along the α_{CL} angle. Spectra were simulated using Simpson with 2000 REPULSION orientations with the β_{CL} angle aligned to the specified value. A RQC of 40.0Hz was used and a quadrupolar asymmetry, η , of 0.0 (left panel) or 1.0 (right panel) were used. The spectra were apodized with 1.0 Hz of exponential line broadening before Fourier Transformation.

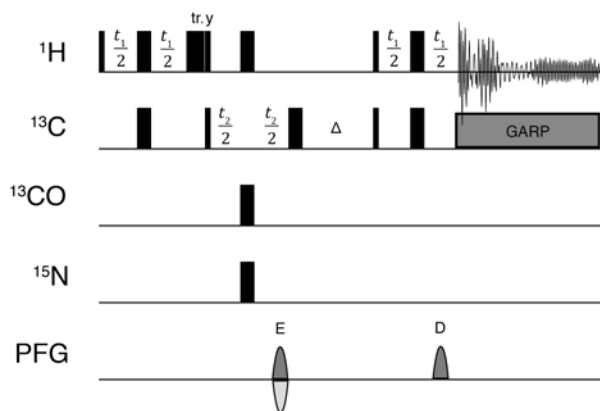


Figure S2. Pulse sequence for the SLF-¹³C-HSQC. The {¹H-¹³C} INEPT and reverse INEPT periods were incremented together in a separate dimension (F1), producing a $\sin^2(\pi J_{CH}t_1)$ or $\sin^2(\pi(J_{CH} + \delta_{CH})t_1)$ signal modulation. The pulse sequence includes a trim pulse (tr.) and gradient encoding (E) and decoding (D) pulses. The period Δ was equal to the initial t_1 duration.

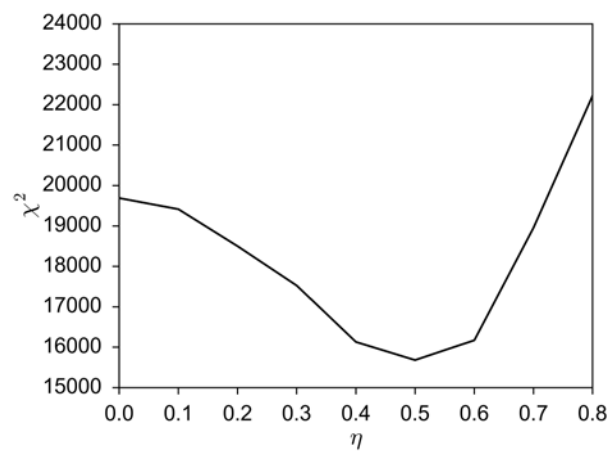


Figure S3. The χ^2 fit for the asymmetry (η) of the $^{13}\text{C}'$ RCSA tensor from the SLF-HA(CA)CO spectrum of PRO ^{13}C , ^{15}N -L-aspartate at pH 5.2 in $^2\text{H}_2\text{O}$ sample. All other parameters ($\delta_{\text{iso,C}'}$, δ_{CH} , $\delta_{\text{C}'}$, β , γ , l_{bCH} , $l_{\text{bC}'}$) were minimized for every η point. See the Experimental Section for sample and experimental details.

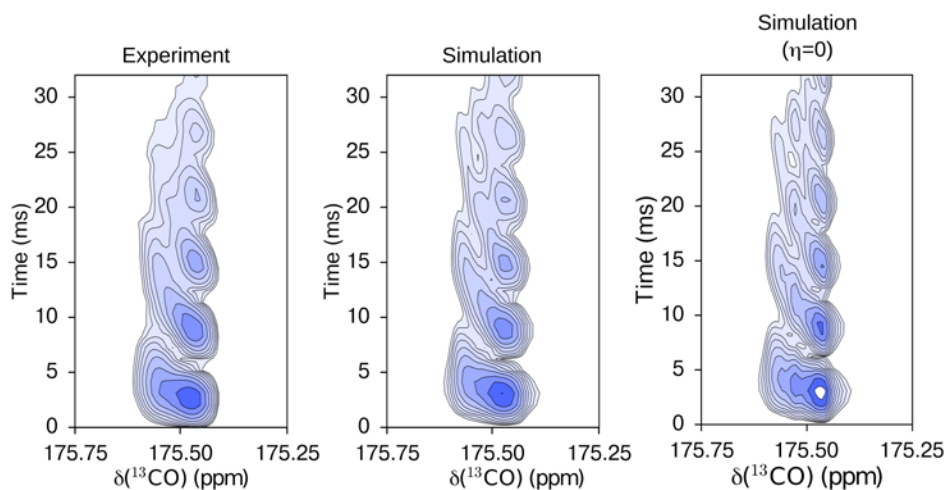


Figure S4. Comparison of the experimental and simulated spectra of the $\{^1\text{H}^\alpha\text{-}^{13}\text{C}^\alpha\}/^{13}\text{C}'$ 2D projection of a SLF-HA(CA)CO spectrum for the PRO ^{13}C , ^{15}N -L-aspartate at pD 5.2 in $^2\text{H}_2\text{O}$. The two simulated spectra represent the best-fit spectrum with a $^{13}\text{C}'$ RCSA tensor asymmetry of $\eta_{\text{C}'} = 0.50 \pm 0.01$ ($\chi^2=15408$) as well as the spectrum with a fixed $\eta_{\text{C}'} = 0.0$ ($\chi^2=19690$).

Table S1. F-tests and quality of fits for the SLF-HACACO of ^{13}C , ^{15}N -L-aspartate in $^2\text{H}_2\text{O}$.

Free Parameters	Number of free parameters	χ^2	χ^2_{red}	F-test P-value (%)
$\delta_{\text{iso,C}'}$, $\text{lb}_{\text{C}'}$, $\text{lb}_{\text{H-C}}$	3	139,798	34.1	0.00%
$\delta_{\text{iso,C}'}$, $\text{lb}_{\text{C}'}$, $\text{lb}_{\text{H-C}}$, δ_{CH}	4	75,440	18.4	0.00%
$\delta_{\text{iso,C}'}$, $\text{lb}_{\text{C}'}$, $\text{lb}_{\text{H-C}}$, δ_{CH} , η_{CH}	5	75,440	18.4	100.0%
$\delta_{\text{iso,C}'}$, $\text{lb}_{\text{C}'}$, $\text{lb}_{\text{H-C}}$, δ_{CH} , $\delta_{\text{C}'}$	5	24,577	6.0	0.00%
$\delta_{\text{iso,C}'}$, $\text{lb}_{\text{C}'}$, $\text{lb}_{\text{H-C}}$, δ_{CH} , $\delta_{\text{C}'}$, $\eta_{\text{C}'}$	6	21,075	5.2	0.00%
$\delta_{\text{iso,C}'}$, $\text{lb}_{\text{C}'}$, $\text{lb}_{\text{H-C}}$, δ_{CH} , $\delta_{\text{C}'}$, $\eta_{\text{C}'}$, β	7	21,018	5.1	0.09%
$\delta_{\text{iso,C}'}$, $\text{lb}_{\text{C}'}$, $\text{lb}_{\text{H-C}}$, δ_{CH} , $\delta_{\text{C}'}$, $\eta_{\text{C}'}$, β , γ	8	20,576	5.0	0.00%